### Title

Evidence for high-temperature fractionation of lithium isotopes during differentiation of the Moon




### Journal

Meteoritics and Planetary Science, 51(6)

### ISSN

1086-9379



### Authors

Day, James MD
Qiu, Lin
Ash, Richard D
et al.



### Publication Date

2016-06-01

### DOI

10.1111/maps.12643

Peer reviewed

The Meteoritical Society

*Meteoritics & Planetary Science* 51, Nr 6, 1046–1062 (2016)
doi: 10.1111/maps.12643

# Evidence for high-temperature fractionation of lithium isotopes during differentiation of the Moon

James M. D. DAY[1*], Lin QIU[2,3], Richard D. ASH[2], William F. McDONOUGH[2], Fang-Zhen TENG[4], Roberta L. RUDNICK[2,6], and Lawrence A. TAYLOR[5]

[1]Geosciences Research Division, Scripps Institution of Oceanography, University of California San Diego, La Jolla, California 92093–0244, USA
[2]Department of Geology, University of Maryland, College Park, Maryland 20740, USA
[3]Department of Geology and Geophysics, Yale University, New Haven, Connecticut 06511, USA
[4]Department of Earth and Space Sciences, University of Washington, Seattle, Washington 98195, USA
[5]Department of Earth and Planetary Sciences, University of Tennessee, Knoxville, Tennessee 37996, USA
[6]Present address: Department of Earth Science, University of California, Santa Barbara, California 93106–9630, USA
[*]Corresponding author. E-mail: jmdday@ucsd.edu

*(Received 20 October 2015; revision accepted 01 March 2016)*

**Abstract**–Lithium isotope and abundance data are reported for Apollo 15 and 17 mare basalts and the LaPaz low-Ti mare basalt meteorites, along with lithium isotope data for carbonaceous, ordinary, and enstatite chondrites, and chondrules from the Allende CV3 meteorite. Apollo 15 low-Ti mare basalts have lower Li contents and lower $\delta^7$Li ($3.8 \pm 1.2$‰; all uncertainties are 2 standard deviations) than Apollo 17 high-Ti mare basalts ($\delta^7\text{Li} = 5.2 \pm 1.2$‰), with evolved LaPaz mare basalts having high Li contents, but similar low $\delta^7$Li ($3.7 \pm 0.5$‰) to Apollo 15 mare basalts. In low-Ti mare basalt 15555, the highest concentrations of Li occur in late-stage tridymite (>20 ppm) and plagioclase ($11 \pm 3$ ppm), with olivine ($6.1 \pm 3.8$ ppm), pyroxene ($4.2 \pm 1.6$ ppm), and ilmenite ($0.8 \pm 0.7$ ppm) having lower Li concentrations. Values of $\delta^7$Li in low- and high-Ti mare basalt sources broadly correlate negatively with $^{18}O/^{16}O$ and positively with $^{56}Fe/^{54}Fe$ (low-Ti: $\delta^7\text{Li} \leq 4$‰; $\delta^{56}\text{Fe} \leq 0.04$‰; $\delta^{18}\text{O} \geq 5.7$‰; high-Ti: $\delta^7\text{Li} > 6$‰; $\delta^{56}\text{Fe} > 0.18$‰; $\delta^{18}\text{O} < 5.4$‰). Lithium does not appear to have acted as a volatile element during planetary formation, with subequal Li contents in mare basalts compared with terrestrial, martian, or vestan basaltic rocks. Observed Li isotopic fractionations in mare basalts can potentially be explained through large-degree, high-temperature igneous differentiation of their source regions. Progressive magma ocean crystallization led to enrichment in Li and $\delta^7$Li in late-stage liquids, probably as a consequence of preferential retention of $^7$Li and Li in the melt relative to crystallizing solids. Lithium isotopic fractionation has not been observed during extensive differentiation in terrestrial magmatic systems and may only be recognizable during extensive planetary magmatic differentiation under volatile-poor conditions, as expected for the lunar magma ocean. Our new analyses of chondrites show that they have $\delta^7$Li ranging between −2.5‰ and 4‰. The higher $\delta^7$Li in planetary basalts than in the compilation of chondrites ($2.1 \pm 1.3$‰) demonstrates that differentiated planetary basalts are, on average, isotopically heavier than most chondrites.

## INTRODUCTION

Lithium is the lightest lithophile element, possessing two stable isotopes, $^6$Li (~7.5% of the natural isotopic abundance) and $^7$Li (~92.5%), with a mass difference of 16%, leading to significant isotopic fractionation in nature (~60‰ in $^7Li/^6Li$, reported as $\delta^7\text{Li} = [(^7Li/^6Li)_{\text{sample}}/(^7Li/^6Li)_{\text{L-SVEC standard}} - 1] \times 1000$) (e.g., Chan and Edmond 1988; Huh et al. 2001; Elliott et al. 2004; Tomascak 2004). Potentially large isotopic fractionations

and mobility in aqueous fluids (e.g., Teng et al. 2006; Liu et al. 2010a) make Li useful for understanding magmatic, metamorphic and hydrothermal processes (e.g., Zack et al. 2003; Elliott et al. 2006; Qiu et al. 2011; Liu et al. 2013). The fractionation behavior of Li isotopes during high-temperature igneous differentiation processes, however, is not well understood. Two prior studies of $^{7}Li/^{6}Li$ systematics during high-temperature magmatic differentiation in terrestrial settings recorded no observable systematic fractionations (e.g., Tomascak et al. 1999; Schuessler et al. 2009).

A number of processes can potentially affect Li isotopes in igneous systems. One is that Li isotope composition can be modified by diffusive processes during interaction between rocks and fluids, modifying original magmatic values (Teng et al. 2006; Liu et al. 2010a). The Li isotopic composition of lunar mare basalts is, however, unlikely to be influenced in this way, given evidence for a volatile-poor source for mare basalts (Sharp et al. 2010; Paniello et al. 2012; Day and Moynier 2014; Kato et al. 2015), and the absence of aqueous fluid alteration on the Moon (e.g., Shearer et al. 2014). A second process is that solid-state diffusion can lead to isotopic fractionation at high temperature. The effects of this process are only preserved if diffusion is followed by rapid quenching. Given sufficient time, such kinetic fractionation will be obliterated by diffusive equilibration (Barrat et al. 2005; Beck et al. 2006; Jeffcoate et al. 2007; Parkinson et al. 2007). Kinetic isotopic fractionations can be significant at the mineral scale, but are less significant at the whole-rock scale, which generally preserves the bulk composition of the system during crystallization and cooling of basaltic flows (Magna et al. 2015). Thus, most basaltic rocks are assumed to reflect the Li isotopic characteristics of their parental melts.

Study of Li isotope variations in lunar mare basalts can potentially shed light on equilibrium isotopic fractionation during magmatic differentiation. This is because mare basalts are considered to form from partial melts of cumulate mineral sources generated during crystallization of a lunar magma ocean (e.g., Wood et al. 1970; Smith et al. 1970; Snyder et al. 1992; Warren and Taylor 2014). Prior studies have investigated high-temperature fractionation effects for O (Spicuzza et al. 2007), Fe (Poitrasson et al. 2004; Weyer et al. 2005; Liu et al. 2010b), Si (Poitrasson and Zambardi 2015), and Mg isotopes (Wiechert and Halliday 2007; Sedaghatpour et al. 2013). These studies have demonstrated that isotopic differences exist between low- and high-Ti mare basalts. In general, these isotopic differences measured in mare basalts have been interpreted to result from inheritance from mineralogically diverse mantle sources generated during lunar magma ocean crystallization.

Studies of Li isotopes in bulk-rock mare basalts have been performed previously, revealing relatively large ranges in $\delta^{7}Li$ (~3‰ total range; Magna et al. 2006; Seitz et al. 2006). However, no prior study of Li isotopes in the Moon has explicitly examined isotopic fractionation during high-temperature differentiation. Here, we investigate well-characterized aliquots of low- and high-Ti mare basalts with the aim of identifying whether Li isotopic fractionation occurred during high-temperature igneous processes in the Moon. A major advantage of our approach is that O and Fe isotopes have previously been measured (Spicuzza et al. 2007; Liu et al. 2010b, respectively) on exactly the same aliquots of material that we have analyzed for Li abundance and isotopic systematics. These data are complemented with in situ Li abundance determinations of mineral grains in Apollo low-Ti mare basalt 15555. Also presented are new Li isotopic measurements of a range of whole-rock chondritic meteorites and chondrule fragments separated from the Allende meteorite. These data are reported in order to allow reexamination of the Li isotope composition of potential planetary building blocks for comparison with lunar Li isotope data.

## SAMPLES

Lunar mare basalts investigated in this study include seven Apollo 15 low-Ti basalts ($TiO_2$ = 1.2–2.3 wt%), six Apollo 17 high-Ti basalts ($TiO_2$ = 11.8–13.2 wt%), and four individual stones of the paired LaPaz (LAP) mare basalt meteorites (LAP 02205/02224/02436/04481), which have experienced limited terrestrial weathering (e.g., Day et al. 2006). Using the definition of Neal and Taylor (1992), all mare basalts in this study are low-Al (<11 wt% $Al_2O_3$) and low-K (<0.2 wt% $K_2O$). Petrology and geochemistry, including highly siderophile element abundances and Os, O, and Fe isotopic compositions, have been reported for the same bulk-rock fragments and/or associated polished sections (Day et al. 2006, 2007; Day and Taylor 2007; Spicuzza et al. 2007; Schnare et al. 2008; Hill et al. 2009; Liu et al. 2010b; Day and Walker 2015). For in situ measurement of Li abundances in mineral grains, new measurements were performed on a thick section of Apollo 15 low-Ti basalt 15555, 955, employed previously in the study by Schnare et al. (2008).

Apollo 15 mare basalts include both olivine-normative basalts and quartz-normative basalts that are potentially linked through crystal fractionation processes (Schnare et al. 2008) and partial melting of

mantle source regions (e.g., Chappell and Green 1973; Rhodes and Hubbard 1973). Apollo 17 mare basalts include A-, B-, C-, and U-types that are grouped by their differences in mineralogy and chemical composition (Neal and Taylor 1992); for example, A-type basalts have higher Sm concentrations than that of B- and C-types, and C-type basalts have lower Rb/Ba than those of A- and B-type basalts. Apollo 17 mare basalts that do not fall into readily defined groupings are considered U-type (Neal and Taylor 1992). Relative to Apollo 15 low-Ti mare basalts, Apollo 17 high-Ti mare basalts contain high modal abundances of ilmenite and armalcolite. Parental melts of LaPaz mare basalts were probably similar to those of the Apollo 12 low-Ti basalts, but experienced significant closed-system fractionation of olivine and chromite (e.g., Righter et al. 2005; Zeigler et al. 2005; Anand et al. 2006; Day et al. 2006). Enrichment of the incompatible elements in the LaPaz basalts, however, indicates that they cannot be directly related to an Apollo mare basalt suite and instead, possess a KREEP-like (K, REE, P, U, Th) component inherited from their source(s) (Day et al. 2006; Rankenburg et al. 2007).

Chondrite meteorites examined in this study include 12 carbonaceous chondrites, six ordinary chondrites, and the enstatite chondrite Kota-Kota. These meteorites span the range of major chondrite petrological types. Only two of the meteorites are finds (Efremovka, Kota-Kota), and the rest are falls, minimizing potential terrestrial contamination and hydrous alteration. Five individual chondrule fragments from the CV chondrite meteorite Allende were also measured to investigate Li isotopic variability within a major component forming chondrites.

## METHODS

### Bulk-Rock Li Isotopic and Abundance Measurements

Lithium concentrations and isotopic compositions were determined at the University of Maryland (UMD), College Park. Sample dissolution procedures, column chemistry, instrumental analysis, and external precision are reported in Rudnick et al. (2004) and Teng et al. (2006). Briefly, for mare basalt samples, 20–60 mg of sample powder, prepared previously (Day et al. 2007), was dissolved in a combination of HF–$HNO_3$–HCl for >72 h at 150 °C until clear solutions were obtained. For chondrites and chondrules, samples were prepared by grinding to fine flour using an agate pestle and mortar. Milligram to 25 mg chondrite and chondrule sample aliquots were then digested in an HF–$HNO_3$ mixture, followed by introduction of $HClO_4$, in high-pressure Teflon digestion vessels, to ensure complete sample dissolution. The amount of sample powder required for analysis was based on Li abundances in whole rocks determined by inductively coupled plasma-mass spectrometry (ICP-MS), with the goal of obtaining 250 ng of Li for multiple analyses of 50 ng solutions for Li abundance and isotope ratio determination. Lithium was purified on cation exchange resin (Bio-Rad AG50w-X12, 200–400 mesh), using two separate column procedures, with the first in HCl, followed by HCl ethanol. Lithium concentrations and isotopic compositions were analyzed using a standard-bracketing methodology on a Nu Plasma multicollector inductively coupled plasma-mass spectrometer (MC-ICP-MS), with L-SVEC lithium carbonate as the standard (Flesch et al. 1973).

The long-term external precision of the Li isotopic composition and concentration analyses at UMD are equal to, or better than 1‰ (2σ) and ±10% (2σ), respectively, based on repeat analyses of pure Li standards and standard reference materials over >10 yr (Tables S1–S3) (Rudnick et al. 2004; Teng et al. 2006; Qiu et al. 2011; Liu et al. 2013). During the course of this study, ten and three separate analyses of basalt standards BHVO-2 and JB-2, respectively, were performed. The average result for analyses of individual digestions of BHVO-2 was $\delta^7Li = 4.3 \pm 0.3‰$ (2σ) and [Li] = 4.7 ± 0.7 ppm (2σ), and the average results for JB2 was $\delta^7Li = 4.0 \pm 0.1‰$ (2σ) and [Li] = 8.7 ± 0.7 ppm (2σ; Table S2). These values are within the range of compositions reported for BHVO-2 ($\delta^7Li$ = 4.0–4.9‰, [Li] = 4.8 ± 0.2 ppm, $n$ = 25) and JB2 ($\delta^7Li$ = 3.6–5.7‰, [Li] = 7.2–8.5 ppm, $n$ = 32) selected by GEOREM (Jochum and Nohl 2008), and through an updated compilation of literature data (BHVO-2: average $\delta^7Li = 4.5 \pm 0.6‰$; average [Li] = 4.5 ± 0.6 ppm; JB2: average $\delta^7Li = 4.7 \pm 1.2‰$; average [Li] = 7.8 ± 0.8 ppm; Table S3). Six total procedural blanks prepared with the samples gave [Li] = 0.2 ± 0.1 ng (2σ), which is negligible relative to the lithium concentration in the samples (blank contributions = <0.1%).

### Lithium Abundance Measurements in Minerals by LA-ICP-MS

To determine the concentration of Li within mineral grains, laser-ablation inductively coupled mass spectrometry (LA-ICP-MS) analyses were performed on a thick section of 15555, 955. This sample was selected for analysis as it is relatively coarse grained, contains well-distinguished oxide and silicate mineral phases, and has been well documented, being the subject of a prior bulk-rock and mineral-scale study (e.g., Schnare et al. 2008). Concentrations of Li were determined using a

New Wave Research UP213 (213 nm) laser-ablation system coupled to a Thermo-Finnigan Element 2 ICP-MS at the University of Maryland. Olivine, pyroxene, plagioclase, ilmenite, and tridymite were analyzed using individual spots with a 30–80 μm-diameter, a laser repetition rate of 7 Hz, and a photon fluence of 2–3.9 J $cm^{-2}$. ThO/Th production was 0.06% for the analytical session. Ablation analysis took place in a 3-$cm^3$ ablation cell. The cell was flushed with a He gas flow of ~0.6 L $min^{-1}$ to enhance production and transport of fine aerosols, and the He gas was mixed with an Ar carrier gas flow of ~0.8 L $min^{-1}$, before reaching the torch. Each analysis consisted of ~60 s data collection. Backgrounds on the sample gas were collected for ~20 s followed by ~40 s of laser ablation. Washout time between spots was >120 s. Data were collected in time-resolved mode, so effects of inclusions, mineral zoning, and possible penetration of the laser beam to underlying phases could be evaluated. Plots of counts per second versus time were examined for each analysis, and integration intervals for the gas background and the sample analysis were selected using LAM-TRACE software. Each LA-ICP-MS analysis was normalized to values of $SiO_2$ (silicates) and $TiO_2$ (oxides) measured by electron microprobe analysis. LA-ICP-MS time-resolved patterns showed that the ablated volumes were homogeneous. Replicate LA-ICP-MS analyses of the BHVO-2 g standard run twice at the beginning and end of analytical sessions as an "unknown" yielded 4.3 ± 0.2 ppm Li (2σ; 4.4 ± 0.8 ppm; Jochum and Nohl 2008) and an external precision of better than ±4% (2σ).

## RESULTS

### Chondrite and Chondrule Li Isotope Systematics

Lithium isotopic compositions of a variety of chondrites and chondrule fragments in Allende are presented in Table 1 and Fig. 1. The $\delta^7$Li of chondrites falls on a near-normal distribution, with an average of 2.1 ± 1.3‰ (2σ, $n$ = 66). In general, carbonaceous chondrites are isotopically heavier than ordinary or enstatite chondrites. The similar composition of Allende chondrules (1 ± 2‰; 2σ, $n$ = 5) with their associated bulk rock (1.6‰) implies that $\delta^7$Li is homogeneous within individual components of at least some fragments of chondrite meteorites (Chaussidon and Robert 1998; Maruyama et al. 2009; Seitz et al. 2012). This is in contrast to the ~50‰ range observed within chondrules from Semarkona (LL3), coupled with an isotopically heavy calculated bulk composition of +10‰ (Chaussidon and Robert 1998). Collectively, these observations are consistent with significant heterogeneity at small scales in some chondrites and chondrite components (e.g., Pogge von Strandmann et al. 2011).

Table 1. Lithium isotopic composition of chondrites.

| Sample | Group | Type[a] | Shock-stage | Fall/Find | $\delta^7$Li |
|---|---|---|---|---|---|
| Orgueil | CI | 1 | – | Fall | 3.9 |
| Ivuna | CI | 1 | – | Fall | 3.0 |
| Murchison | CM | 2 | S1–S2 | Fall | 2.8 |
| Murray | CM | 2 | S1 | Fall | 0.7 |
| Ornans | CO | 3.1 | S1 | Fall | 1.3 |
| Kainsaz | CO | 3.1 | S1 | Fall | 0.5 |
| Felix | CO | 3.4 | S3 | Fall | 2.0 |
| Kaba | CV | 3 | S1 | Fall | 0.7 |
| Allende | CV | 3.2 | S1 | Fall | 1.6 |
| | *Chondrule* | – | – | – | −0.4 |
| | *Chondrule* | – | – | – | 1.0 |
| | *Chondrule* | – | – | – | 1.4 |
| | *Chondrule* | – | – | – | 2.2 |
| | *Chondrule* | – | – | – | 1.0 |
| Efremovka | CV | 3.2 | S4 | Find | 0.4 |
| Vigarano | CV | 3.3 | S1–S2 | Fall | 0.1 |
| Karoonda | CK | 4 | S1 | Fall | 3.2 |
| Krymka | LL | 3.1 | S3 | Fall | −2.5 |
| Chainpur | LL | 3.4 | S1 | Fall | 1.6 |
| Tieschitz | H/L | 3.6 | – | Fall | 1.4 |
| Sharps | H | 3.4 | S3 | Fall | 1.2 |
| Ceniceros | H | 3.7 | – | Fall | 0.8 |
| Dhajala | H | 3.8 | S1 | Fall | 1.5 |
| Kota-Kota | EH | 3 | S4 | Find | −0.9 |

[a]Type 3 samples have been subdivided and the number after the decimal refers to the degree of thermal modification, with higher numbers for more altered samples.

### Lithium Abundances in Mineral Grains from Apollo 15555

Concentrations of Li in plagioclase, olivine, pyroxene, ilmenite, and tridymite analyzed by LA-ICP-MS are presented in Table 2. Plagioclase grains have high Li contents, ranging from 8.2 to 12.7 ppm (Av. = 11.0 ± 3.1 ppm; 2σ, $n$ = 8). Pyroxene (Av. = 4.2 ± 1.6 ppm; 2σ, $n$ = 10) and olivine (Av. = 6.1 ± 3.8 ppm; 2σ, $n$ = 11) grains do not appear to show core-to-rim variations in Li abundances in the mineral grains that were measured. Ilmenite has the lowest observed Li content (Av. = 0.8 ± 0.7 ppm; 2σ, $n$ = 5) in 15555. Only one tridymite grain was successfully measured, with other tridymite grains fragmenting during LA-ICP-MS analysis as a consequence of its poor photon coupling characteristics at these wavelengths. This grain yielded a high Li content (41 ppm), indicating enrichment of Li in the late-stage mesostasis with which tridymite grains are associated.

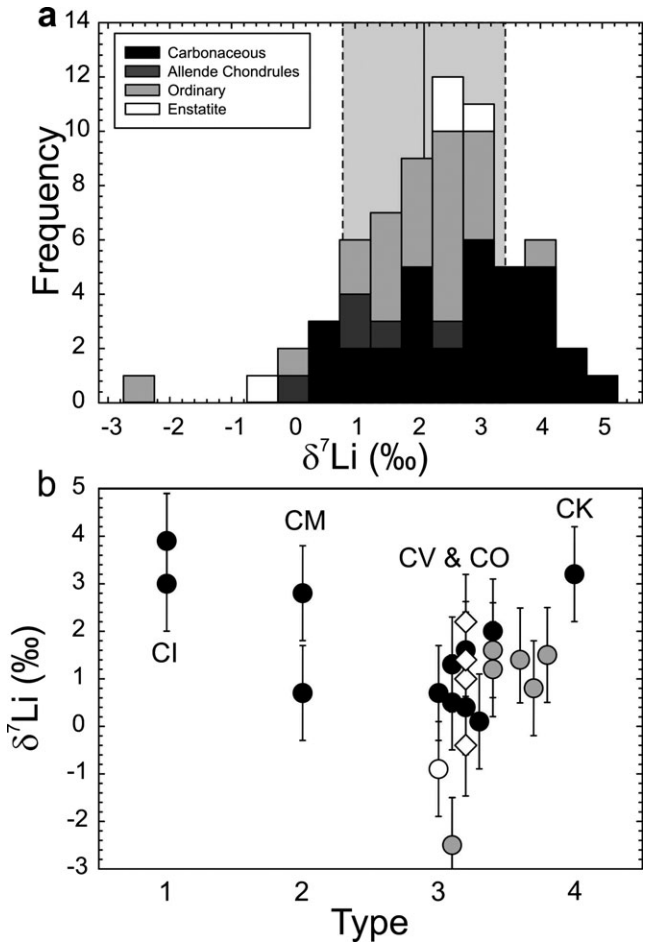


Fig. 1. a) Histogram of $\delta^7$Li values in carbonaceous, ordinary, and enstatite chondrites and Allende chondrules from this study and Seitz et al. (2007). Line and shaded region denotes average and two standard deviation of the compiled data set (2.1 ± 1.3‰). b) $\delta^7$Li versus chondrite type classification for carbonaceous chondrites (filled circles); chondrule components in Allende (unfilled diamonds); ordinary chondrites (gray circles); and the enstatite chondrite, Kota-Kota (unfilled circle), from this study. Error bars in (b) represent long-term external uncertainties for the UMD laboratory (±1‰, 2σ).

## Mare Basalt Lithium Isotope Compositions and Abundances

Lithium isotopic compositions and abundances for mare basalts are reported in Table 3 and in Fig. 2. Apollo 15 samples have between 7 and 8.5 ppm Li and $\delta^7$Li ranging from 3.1‰ to 4.8‰. Apollo 15 quartz-normative basalts have $\delta^7$Li values (QNB = 3.3 ± 0.6‰, 2σ) within uncertainties of Apollo 15 olivine-normative basalts (ONB = 4.2 ± 0.8‰, 2σ) and have similar Li abundances. Apollo 17 high-Ti mare basalts have both higher concentrations of Li than Apollo 15 low-Ti mare basalts, at 8.8–16.5 ppm Li, and are also isotopically heavier ($\delta^7$Li = 4.5–6.2‰). 74255 is isotopically the heaviest mare basalt sample measured ($\delta^7$Li = 6.0 ± 0.5‰, 2σ), but there are no distinguishing differences between other Apollo 17 mare basalt types based on our sampling. Lithium concentrations measured in this study span a similar range as published values for Apollo 15 (4.6–8 ppm) and Apollo 17 (7–11.4 ppm) mare basalts (Meyer 2012). LaPaz mare basalts have elevated Li contents (11.6–13.8 ppm) with respect to Apollo 15 mare basalts but similar $\delta^7$Li values (3.4–4.1‰) to Apollo 15 QNB. Combined, the new data for high-Ti and low-Ti mare basalts give average $\delta^7$Li of 5.1 ± 1.1‰ and 3.6 ± 0.6‰ (2σ), respectively. An unpaired Student *t*-test yields a two-tailed *P*-value of less than 0.0001, indicating statistical significance and rejection of the hypothesis that low- and high-Ti mare basalts that were measured have similar $\delta^7$Li values.

Two studies have previously reported Li isotope and abundance data for mare basalts. Concentration and Li isotopic ratios obtained in this study are similar to those reported by Magna et al. (2006). Conversely, while $\delta^7$Li values overlap those reported by Seitz et al. (2006), the Li concentrations reported in that study are ~30% lower (Fig. 2). Mineralogical heterogeneity between sample aliquots may partly explain these discrepancies, given the variability in Li contents observed within mineral grains of 15555.

Table 2. Lithium abundances in minerals from 15555.

| Sample | Li (ppm) | Sample | Li (ppm) |
|---|---|---|---|
| Area1 Plag1 | 10.4 | Area1 Px1 | 3.4 |
| Area1 Plag1 | 12.1 | Area3 Px1 | 4.7 |
| Area3 Plag1 | 12.7 | Area2 Px | 4.4 |
| Area3 Plag2 | 11.4 | Area5 Px (core) | 4.3 |
| Area2 Plag | 11.1 | Area5 Px (rim) | 5.9 |
| Area6 Pl | 12.4 | Area5 Px (rim) | 4.9 |
| Area7 Plag | 9.3 | Area5 Px (rim) | 3.7 |
| Area10 Plag | 8.2 | Area5 Px (core) | 4.3 |
| *Average Pl* | *11.0* | Area6 Px | 3.5 |
| *2 SD* | *3.1* | Area7 Px | 3.2 |
| | | *Average Px* | *4.2* |
| Area1 Ol1 | 7.7 | *2 SD* | *1.6* |
| Area3 Ol1 | 5.8 | | |
| Area3 Ol2 | 6.9 | Area4 Ilm | 0.4 |
| Area4 Ol1 (edge) | 7.8 | Area2 Ilm | <5.8 |
| Area4 Ol1 (center) | 7.2 | Area2 Ilm | 1.1 |
| Area4 Ol1 (edge) | 7.6 | Area5 Ilm | <1.3 |
| Area2 Ol | 3.7 | Area6 Ilm | 0.8 |
| Area6 Ol | 3.5 | *Average Ilm* | *0.8* |
| Area6 Ol | 4.0 | *2 SD* | *0.7* |
| Area7 Ol | 4.0 | | |
| Area10 Ol | 8.5 | Area6 Trid | 40.8 |
| *Average Ol* | *6.1* | Area6 Trid | <16 |
| *2 SD* | *3.8* | | |

Italics denote averages and standard deviations of data.

Table 3. Lithium isotope and abundance data for mare basalts.

| Sample | Rock type | | $\delta^7$Li | ±2σ | Li (ppm) | ±2σ | $\delta^{18}$O[a] | $\delta^{56}$Fe[a] | MgO (wt%)[b] | $TiO_2$ (wt%)[b] | Olivine[b] | Pyroxene[b] | Ilm + Ulvo[b] | Plagioclase[b] | "Mesostasis"[b] | Exposure Age (Ma)[b] |
|---|---|---|---|---|---|---|---|---|---|---|---|---|---|---|---|---|
| Apollo 15 mare basalts | | | | | | | | | | | | | | | | |
| 15475, 187 | QNB | | 3.1 | | 7.4 | | | | | | | | | | | |
| | | | 3.3 | | 7.6 | | | | | | | | | | | |
| | | | 3.2 | | 7.4 | | | | | | | | | | | |
| | | *Av.* | *3.2* | *0.2* | *7.4* | *0.2* | 5.682 | 0.038 | 10.6 | 1.2 | 0.6 | 59.7 | 1.7 | 30.2 | 7.8 | 543 ± 183 |
| | *15475* (Magna et al. 2006) | | *3.4* | | *7.2* | | | | | | | | | | | |
| 15596, 24 | QNB | | 3.5 | | 8.5 | | | | | | | | | | | |
| | | | 4.0 | | 8.0 | | | | | | | | | | | |
| | | *Av.* | *3.7* | *0.7* | *8.2* | *0.7* | 5.602 | – | 9.0 | 1.7 | 4 | 48 | 1 | 35 | 12 | – |
| 15499, 154 | QNB | | 3.1 | | 7.5 | | | | | | | | | | | |
| | | | 3.1 | | 7.7 | | | | | | | | | | | |
| | | *Av.* | *3.1* | *0.1* | *7.6* | *0.3* | 5.693 | – | 7.9 | 1.9 | 1.9 | 80.7 | 1.9 | 13.1 | 2.4 | 114 |
| 15016. 221 | ONB | | 4.2 | | 8.2 | | | | | | | | | | | |
| | | | 4.8 | | 7.4 | | | | | | | | | | | |
| | | *Av.* | *4.5* | *0.8* | *7.8* | *1.1* | 5.616 | 0.067 | 12.3 | 2.3 | 14.5 | 58.9 | 3.6 | 20.9 | 2.1 | 285–315 |
| 15555, 950 | ONB | | 4.4 | | 8.4 | | | | | | | | | | | |
| | | | 3.9 | | 8.0 | | | | | | | | | | | |
| | | *Av.* | *4.2* | *0.7* | *8.2* | *0.5* | 5.443 | *0.073* | 11.3 | 1.8 | 14.7 | 53.2 | 3.6 | 23.7 | 4.8 | 76–90 |
| 15555, 955 | ONB | | 4.3 | | 7.0 | | | | | | | | | | | |
| | | | 3.9 | | 7.3 | | | | | | | | | | | |
| | | *Av.* | *4.1* | *0.5* | *7.2* | *0.4* | 5.631 | 0.073 | 11.7 | 1.8 | 14.7 | 53.2 | 3.6 | 23.7 | 4.8 | 76–90 |
| 15555, 958 | ONB | | 3.7 | | 7.1 | | | | | | | | | | | |
| | | | 4.8 | | 7.4 | | | | | | | | | | | |
| | | *Av.* | *4.2* | *1.6* | *7.3* | *0.4* | 5.769 | *0.073* | 12.8 | 1.4 | 14.7 | 53.2 | 3.6 | 23.7 | 4.8 | 76–90 |
| | *15555* (Seitz et al. 2006) | | *3.6* | | *5.8* | | | | | | | | | | | |
| | *15555* (Magna et al. 2006) | | *4.3* | | *6.0* | | | | | | | | | | | |
| Apollo 17 mare basalts | | | | | | | | | | | | | | | | |
| 70017, 524 | U-type basalt | | 5.3 | | 10.4 | | | | | | | | | | | |
| | | | 4.8 | | 9.7 | | | | | | | | | | | |
| | | *Av.* | *5.1* | *0.8* | *10.0* | *0.9* | 5.578 | 0.205 | 9.9 | 11.8 | 1.2 | 51.6 | 16.6 | 26 | 4.6 | 220 ± 20 |
| 70035, 180 | U-type basalt | | 4.8 | | 10.0 | | | | | | | | | | | |
| | | | 5.0 | | 10.2 | | | | | | | | | | | |
| | | *Av.* | *4.9* | *0.3* | *10.1* | *0.3* | 5.367 | 0.142 | 9.5 | 15.1 | 1.2 | 45.1 | 17.6 | 35 | 1.1 | 122 ± 3 |
| | *70035* (Magna et al. 2006) | | *5.1* | | *8.6* | | | | | | | | | | | |
| 75075, 171 | B1-type basalt | | 4.9 | | 16.5 | | | | | | | | | | | |
| | | | 4.6 | | 10.3 | | | | | | | | | | | |

Table 3. *Continued.* Lithium isotope and abundance data for mare basalts..

| Sample | Rock type | | $\delta^7$Li | ±2σ | Li (ppm) | ±2σ | $\delta^{18}$O[a] | $\delta^{56}$Fe[a] | MgO (wt%)[b] | $TiO_2$ (wt%)[b] | Olivine[b] | Pyroxene[b] | Ilm + Ulvo[b] | Plagioclase[b] | "Mesostasis"[b] | Exposure Age (Ma)[b] |
|---|---|---|---|---|---|---|---|---|---|---|---|---|---|---|---|---|
| | | *Av.* | *4.7* | *0.4* | *13.4* | *8.7* | 5.335 | 0.217 | 9.4 | 13.3 | <0.1 | 48.5 | 15 | 32.4 | 4.1 | 119–128 |
| | *75075* (Magna et al. 2006) | | *5.3* | | *10.3* | | | | | | | | | | | |
| 70135, 98 | A-type basalt | | 4.5 | | 11.5 | | | | | | | | | | | |
| | | | 5.1 | | 10.7 | | | | | | | | | | | |
| | | *Av.* | *4.8* | *0.9* | *11.1* | *1.2* | 5.591 | | 9.8 | 11.8 | 2.6 | 49.3 | 16 | 29.4 | 2.7 | 106 ± 4 |
| 70215, 322 | B2-type basalt | | 4.5 | | 8.9 | | 5.529 | 0.171 | 7.3 | 12.8 | 7.3 | 40.6 | 14.6 | 33.3 | 4.2 | 100 ± 12 |
| 74255, 185 | C-type basalt | | 5.6 | | 11.4 | | | | | | | | | | | |
| | | | 6.2 | | 10.0 | | | | | | | | | | | |
| | | | 5.9 | | 8.8 | | | | | | | | | | | |
| | | | 6.1 | | 10.2 | | | | | | | | | | | |
| | | *Av.* | *6.0* | *0.3* | *10.1* | *1.5* | 5.407 | 0.182 | 10.5 | 12.8 | 3.5 | 53.2 | 14.2 | 26.6 | 2.5 | 25 ± 3 |
| | *74255* (Magna et al. 2006) | | *6.4* | | *9.2* | | | | | | | | | | | |
| Evolved mare basalt meteorites | | | | | | | | | | | | | | | | |
| LAP 02205, 21 | Evolved mare basalt | | 3.6 | | 12.4 | | | | | | | | | | | |
| | | | 4.1 | | 13.8 | | | | | | | | | | | |
| | | *Av.* | *3.9* | *0.7* | *13.1* | *2.0* | 5.763 | – | 6.3 | 3.1 | 1.6 | 54.6 | 3.8 | 33.4 | 6.6 | 43 ± 7 |
| LAP 02224, 17 | Evolved mare basalt | | 3.7 | | 11.8 | | 5.653 | – | 6.8 | 3.3 | 1.6 | 54.6 | 3.8 | 33.4 | 6.6 | |
| LAP 02436, 20 | Evolved mare basalt | | 3.4 | | 11.7 | | 5.701 | – | 7.7 | 3.2 | 1.6 | 54.6 | 3.8 | 33.4 | 6.6 | |
| LAP 04481, 6 | Evolved mare basalt | | 3.7 | | 11.6 | | – | – | | | 1.5 | 56.2 | 4.2 | 31.9 | 6.2 | |

Replicate analyses of samples are from repeat column chemistry and MC-ICP-MS analysis of samples.

[a]Values of $\delta^{18}$O and $\delta^{56}$Fe are from Spicuzza et al. (2007) and Liu et al. (2010b), respectively.

[b]Mineralogy, MgO (wt%) and $TiO_2$ (wt%) data are from Day et al. (2006) and unpublished data. Exposure ages were compiled from Meyer (2012).

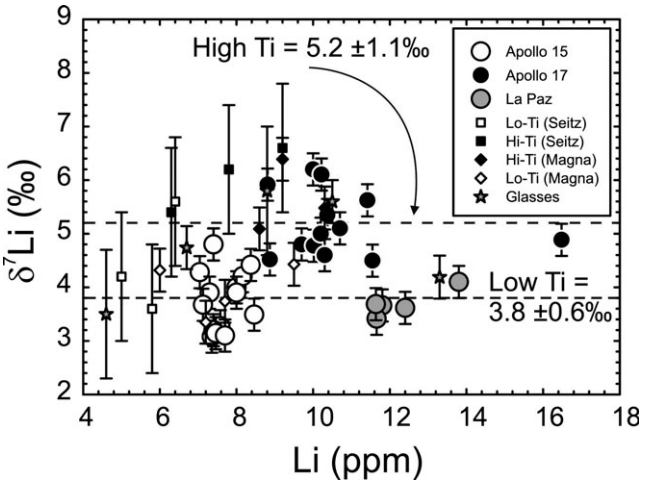


Fig. 2. Li concentration versus $\delta^7$Li for lunar samples from this study showing averages between low- (Apollo 15, LaPaz) and high-Ti mare basalts (Apollo 17) versus data for low- and high-Ti mare basalts and pyroclastic glass beads from Seitz et al. (2006) and Magna et al. (2006). While our lithium isotopic data compare well with data from the two previously published studies, we obtain higher Li abundances than Seitz et al. (2006). The magnitude of difference in $\delta^7$Li between low- and high-Ti mare basalts for all three studies is the same. An unpaired Student *t*-test yields a two-tailed *P*-value of less than 0.0001, indicating statistical significance and rejection of the hypothesis that the low- and high-Ti mare basalts compiled from this study, Magna et al. (2006) and Seitz et al. (2006), have the same $\delta^7$Li values. Error bars denote 2σ uncertainties for samples from the different studies. Long-term external uncertainties for the UMD laboratory are ±1‰ (2σ).

Several of the same samples have been analyzed in previous studies (Magna et al. 2006; Seitz et al. 2006). Data reported for 70035, 74255, and 75075 in Magna et al. (2006) are within analytical uncertainty for both concentration and $\delta^7$Li to those reported here. For the two samples (15475 and 15555) measured by all three studies, $\delta^7$Li values are identical within uncertainties (Table S4).

## DISCUSSION

### Aqueous Alteration and Thermal Modification of Chondrites

While aqueous alteration can be excluded as a process that may have affected the mare basalts, the same is not true for chondrite meteorites. Petrological and geochemical evidence exists for aqueous alteration and thermal modification of chondrite parent bodies early in their formation (Brearley and Jones 1998). The broad relationship of increasing petrological type and lower $\delta^7$Li indicates that parent body processes operative during formation of chondrites (aqueous alteration and/or thermal modification) may have played a role in modification of their Li isotopic ratios (Fig. 1). The results are consistent with prior studies showing that secondary alteration is probably responsible for the range of $\delta^7$Li values observed in chondrites and chondritic components (e.g., Sephton et al. 2004; Seitz et al. 2007, 2012; Maruyama et al. 2009). The high vibrational frequency of water relative to mineral phases (Huh et al. 2001), or stronger tetrahedral bonds in $H_2O$ than octahedral coordination of Li in minerals (Teng et al. 2004) dominates Li isotopic fractionation, leading to preferential partitioning of $^7$Li into water. High $\delta^7$Li in the lowest petrological grade of chondrites (e.g., CI) likely reflects uptake of isotopically heavy Li from water into secondary phases (e.g., Sephton et al. 2013). Kinetic isotopic fractionation effects have been shown to affect the $\delta^7$Li of phenocrysts (e.g., Jeffcoate et al. 2004; Barrat et al. 2005; Beck et al. 2006; Parkinson et al. 2007) and might also have an effect at the scale of chondrules and matrix in chondrites (e.g., Maruyama et al. 2009; Pogge von Strandmann et al. 2011; Seitz et al. 2012). However, the similarity in $\delta^7$Li for the chondrules that we measured in Allende, compared with the bulk sample, suggests equilibration of Li in this particular meteorite.

### Effects on $\delta^7$Li from Secondary Irradiation and Implantation

Significant Li isotopic variations can occur through spallation reactions during exposure of materials to cosmic rays. Both $^6$Li and $^7$Li are produced subequally during spallation, but because $^7$Li is ~12 times more abundant than $^6$Li in rocks, the effect will be to decrease $^7$Li/$^6$Li. Conversely, the presence of implanted solar wind would have an opposing effect to spallation, increasing $\delta^7$Li, due to preferential exhaustion of $^6$Li early in the history of Sun-like stars due to a neutron capture cross section some 20,000 times greater than that of $^7$Li. For example, the solar wind is estimated to have $^7$Li/$^6$Li of ~31 (Chaussidon and Robert 1999), and galactic cosmic-ray-induced reactions have yielded $^7$Li/$^6$Li of between 1 and 2 (Eugster and Bernas 1971; Knauth et al. 2000). While the effect of solar wind implantation would be to increase $\delta^7$Li, the depth of penetration is limited to ~0.01 μm from the surface (Chaussidon and Robert 1999) and has been shown to have negligible effects on chondrites and their components (Seitz et al. 2012). Additionally, Seitz et al. (2012) determined that the majority of chondrules require limited correction due to cosmic-ray exposure, increasing $\delta^7$Li by not more than 1‰, consistent with the generally limited cosmic-ray exposure (CRE) ages

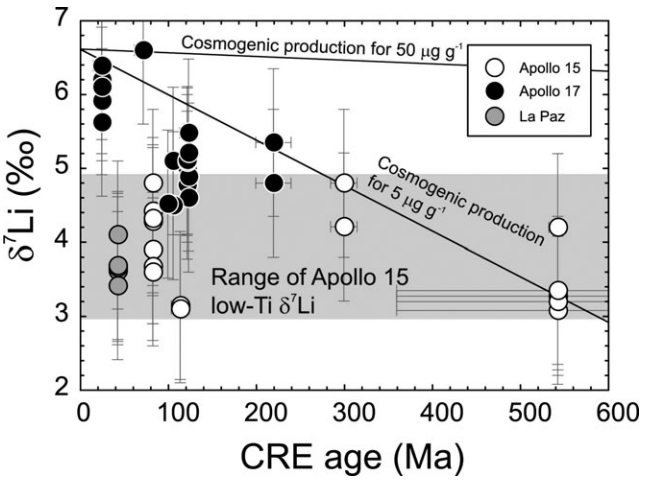


Fig. 3. Comparison of cosmic-ray exposure age (CRE in millions of years from present) versus the $\delta^7$Li of mare basalt samples (this study; Magna et al. 2006; Seitz et al. 2006). Also shown are estimated $\delta^7$Li curves assuming cosmogenic production of $^6$Li at ~0.15 that of $^3$He for rock targets with different initial Li concentrations (after Seitz et al. 2006, 2012). Note the lack of correlation between CRE age and Li isotope composition in low-Ti mare basalts, illustrated by the range of Apollo 15 low-Ti $\delta^7$Li. Uncertainties for CRE ages are given in Table 1 and long-term external uncertainties from the UMD laboratory (±1‰, 2σ) for $\delta^7$Li are shown.

measured for chondrites (<25 Ma; e.g., Eugster et al. 2007).

CRE ages for mare basalts measured in this study range from ~25 Ma to 548 ± 183 Ma (Table 3); the heaviest $\delta^7$Li value is measured in the sample having one of the youngest exposure ages (74255), whereas the sample with the oldest exposure age (15475) has one of the lowest $\delta^7$Li values (Fig. 3). The largest range of exposure ages in samples from a single mission are for Apollo 15 mare basalts (~76 to ~543 Ma); these samples show no correlation between $\delta^7$Li and CRE age. In order to estimate cosmogenic production of $^6$Li, we follow previous assumptions made by Seitz et al. (2006, 2012), assuming a production ratio between $^6$Li and $^3$He of about 0.15 ± 0.50. Using this scaled production of cosmogenic Li and the Li content of lunar samples, it is possible to generate evolution curves for $^7$Li/$^6$Li modification using CRE over time (Fig. 3). The results are in agreement with the conclusions of Seitz et al. (2006) and Magna et al. (2006) that, while some cosmogenic modification can occur over the CRE ages observed in mare basalts, they do not explain the large range in $\delta^7$Li values observed for mare basalts with relatively young CRE ages (e.g., LaPaz, 15555), nor can this process explain the systematic differences observed between low- and high-Ti mare basalts for $\delta^7$Li. We find no evidence that samples analyzed here were systematically modified by secondary irradiation and implantation of lithium.

## Mineralogical Heterogeneity in Mare Basalts and Mantle-Melt Partitioning

Experimental studies have examined partitioning of Li between terrestrial basaltic melts and minerals (e.g., $K_D$ Ol = 0.2–0.4; $K_D$ Pl = 0.3–0.4; $K_D$ Cpx = 0.26–0.75; Brenan et al. 1998); however, few experiments have been performed relevant to lunar conditions (low Na and K, sometimes high Ti; $K_D$ Opx = ~0.2; Van Kan Parker et al. 2011), and no data are currently available for ilmenite or other Fe-Ti oxide phases. Lithium concentrations have been measured in a few minerals in Apollo 11 high-Ti mare basalts and vary from ~11 to 55 ppm in plagioclase, 5–45 ppm in pyroxene, and >10 ppm in ilmenite, with higher concentrations measured in brecciated samples (Andersen et al. 1970). Our new data for Apollo 15555 mineral grains indicate more limited ranges in Li concentration, with 8–13 ppm Li in plagioclase, 3–9 ppm in pyroxene, 3.5–8.5 ppm in olivine, 0.4–1 ppm in ilmenite, but as much as 41 ppm Li in tridymite (Table 2). These results suggest incorporation of Li in lunar minerals in the general order of melt > plagioclase ≥ olivine ≥ pyroxene > ilmenite. While not directly measured using LA-ICP-MS in this study, it is notable that the mineral structure of armalcolite (Mg, $Fe^{2+}$) $Ti_2O_5$ has fourfold coordination of Mg, and so may act as a carrier for Li.

In order to assess the relative distribution of Li in minerals within mare basalts, calculations were performed using the modal abundances of the minerals and the average concentrations of Li measured in 15555 mineral grains, assuming similar concentrations of Li in the minerals of all of the mare basalts (Fig. S1). This exercise serves to demonstrate that modal recombination using only major mineral phases (olivine, pyroxene, plagioclase, ilmenite) does not reproduce most of the measured bulk compositions, which are too high to be explained by Li within these minerals alone. To reproduce the measured Li contents, mesostasis (here assumed to be represented by the modal abundance of 4.8% in Table 2) Li contents of ~20 ppm are required for reasonable fits for Apollo 15 low-Ti mare basalts. Measured Li concentrations in high-Ti mare basalts and the LaPaz mare basalts are higher than modal recombination calculations using the 15555 mineral Li contents. This discrepancy probably reflects high Li contents in Apollo 17 and LaPaz basalts, with the possibility of similar Li enrichment in their mineral phases. Further work is warranted to examine the siting of Li within lunar minerals from a variety of mare basalts.

## No Evidence for Volatile Loss of Li during Planetary Formation and Differentiation

Since Li is an incompatible element that becomes enriched in melts (e.g., Brenan et al. 1998), partial melting leads to approximately order of magnitude higher Li concentrations in terrestrial mid-ocean ridge basalts (MORB) relative to terrestrial peridotite whole rocks and minerals, and a mantle-melt bulk-partitioning of ~0.1. MORB and mare basalts are estimated to be generated by similar degrees of partial melting (≤10%; cf. Plank and Langmuir 1992; Snyder et al. 1997), with 5–11% partial melting estimated for mare basalt sources (Day and Walker 2015). The similarity in Li contents between terrestrial basalts and mare basalts, as well as with eucrites and shergottites (e.g., Mittlefehldt 2005; Magna et al. 2015), implies that the Li contents of their respective planetary mantles are subequal. Some consistency therefore appears to exist in Li abundances between planets, with similar Li abundances observed between bulk-rock terrestrial peridotites and chondrites. The majority of whole-rock terrestrial peridotites and mantle-derived melts from Earth, Mars, and Vesta and the low-Ti mare basalts have $\delta^7$Li within the range of the bulk silicate Earth estimate (Fig. 4). However, a striking aspect of Li isotopes in mare basalts is that high-Ti mare basalts have systematically higher Li concentrations and are isotopically heavier than low-Ti mare basalts. These results are inconsistent with volatile depletion of Li to explain $\delta^7$Li enrichment. During volatile depletion, Li concentrations would be expected to decrease as $^7$Li/$^6$Li increases, due to kinetic isotopic fractionation, as has been observed for moderately volatile elements (Day and Moynier 2014). Similarity in Li contents for melt products from the Moon, Earth, Mars, and some asteroids implies that Li experienced limited depletion as a moderately volatile element (50% condensation temperature = 1142 K) during planetary accretion and differentiation.

## Evidence for Global-Scale Isotopic Fractionation of Lithium

The new Li isotope results support significant differences in $\delta^7$Li between low- and high-Ti mare basalts, as indicated previously (Magna et al. 2006; Seitz et al. 2006). Since the same sample aliquots measured for Li in this study have also been measured for O and Fe isotopes (Spicuzza et al. 2007; Liu et al. 2010b), it is possible to examine whether there are coherent variations in Li, O, and Fe stable isotopes (Fig. 5). The $\delta^7$Li values of lunar basalts negatively correlate with $^{18}$O/$^{16}$O and positively correlate with $^{56}$Fe/$^{54}$Fe. These trends may reflect a source with low-

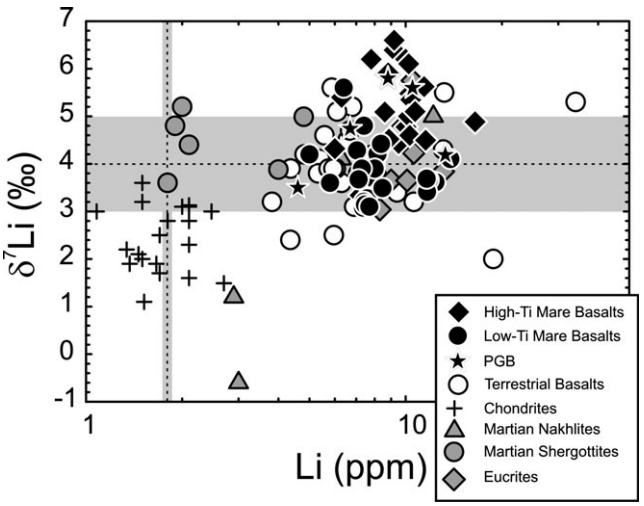


Fig. 4. Lithium abundance and isotopic compositions for basalts from Earth, Mars, the Moon, and the eucrite parent body(ies), compared with nakhlites (Mars), lunar pyroclastic glass beads, and chondrites. Basaltic rocks from Earth, Mars, the Moon, and the eucrite parent body all appear to have similar ranges in $\delta^7$Li, but are on average above chondritic materials. Data are from Seitz et al. (2004, 2006, 2007, 2012), Elliott et al. (2006), Magna et al. (2006, 2008, 2014), Tomascak et al. (2008), and this study. Gray boxes indicate the estimated compositional averages for the bulk silicate Earth (from Seitz et al. 2007). Uncertainties are generally ±1‰ (2σ) for $\delta^7$Li.

$\delta^7$Li (≤4‰), low-$\delta^{56}$Fe (≤0.04‰), and high-$\delta^{18}$O (≥5.7‰) that is most effectively sampled by low-Ti mare basalts. A source with higher $\delta^7$Li (>6‰), $\delta^{56}$Fe (>0.18‰), and low-$\delta^{18}$O (<5.4‰) is required for high-Ti mare basalts. The most logical explanation for these differences is that the sources for the high- and low-Ti mare basalts were mineralogically different and that these sources experienced distinct and measurable Li, O, and Fe isotopic fractionation.

A long-term paradigm for lunar evolution has been early wholesale melting of the Moon and subsequent crystallization of a magma ocean (e.g., Smith et al. 1970; Wood et al. 1970). It has been demonstrated that progressive fractionation of mafic silicates occurred in a magma ocean until plagioclase saturation was reached at ~80% crystallization, with dense Fe-Ti oxides precipitating at ~95% crystallization (Snyder et al. 1992). Models of magma ocean stratification envisage early olivine and pyroxene cumulates, followed by a plagioclase-rich crust, formed by flotation. Under this cover, Fe-Ti oxides and late-stage incompatible-rich segregations accumulated (so-called primordial potassium, rare Earth element, phosphorous [KREEP], or urKREEP; e.g., Shearer and Papike 1999; Warren and Taylor 2014). The presence of nearly ubiquitous negative Eu anomalies in mare basalts, indicating

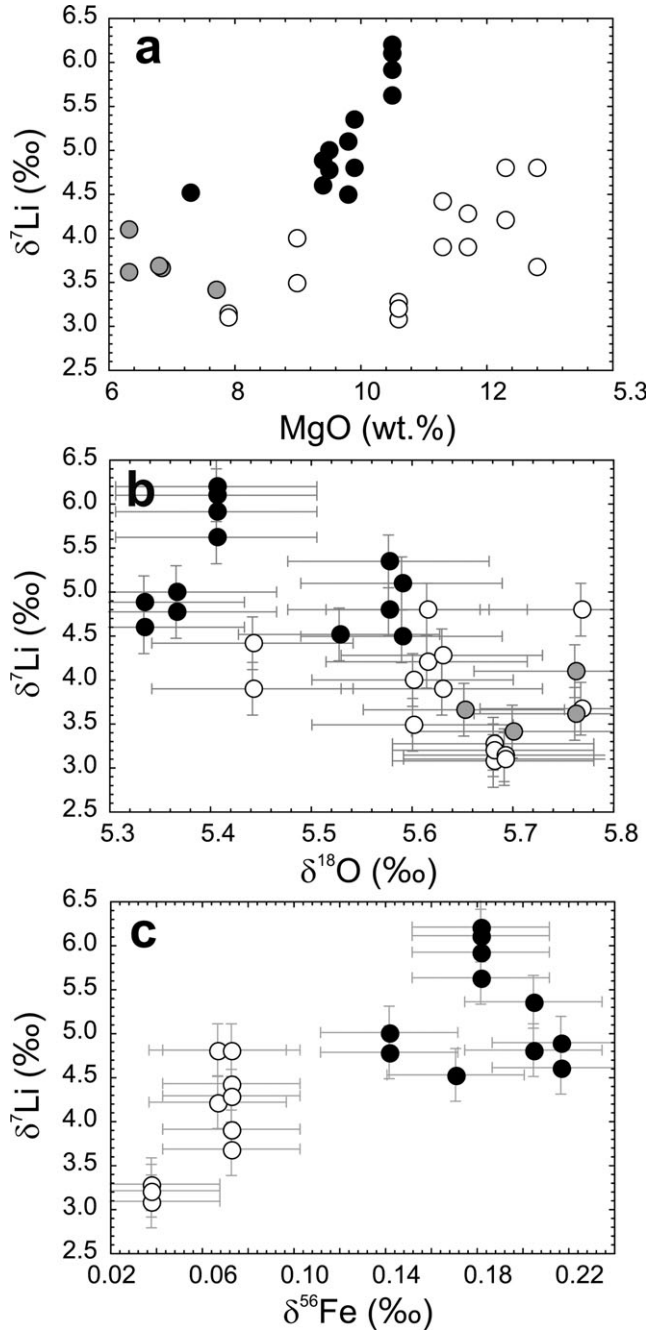


Fig. 5. Bulk rock lithium isotopic composition versus (a) MgO content, (b) $\delta^{18}O$, and (c) $\delta^{56}Fe$. Oxygen and iron isotope data are from Spicuzza et al. (2007) and Liu et al. (2010b), respectively. Uncertainties shown in (b) and (c) for $\delta^7Li$ are the $2\sigma$ external precision from this study, and uncertainties for O and Fe given in Spicuzza et al. (2007) and Liu et al. (2010b), respectively.

plagioclase extraction, and the presence of high-Ti mare basalts equilibrated at depths >200 km (below the theoretical saturation point of Fe-Ti oxides in a magma ocean scenario), have also led to modified models of magma overturn and imperfect mixing of the cumulate pile to explain the distribution of mantle sources (e.g., Elkins-Tanton et al. 2002).

Using a magma ocean crystallization model (Snyder et al. 1992), we calculate theoretical Li isotopic fractionation as a Rayleigh distillation process, with preferential partitioning of $^6Li$ into crystallizing mafic silicate minerals. Due to the lack of experimentally determined fractionation factors that can be used for such a calculation, a number of assumptions have been made. First, the calculation assumes an enrichment of $^7Li$ in melt relative to mineral phases during progressive fractional crystallization, leading to preferential retention of $^6Li$ in the solid phase. The theoretical basis for this variation is due to higher bond strength of Li in tetrahedral coordination in the melt relative to octahedral coordination of Li in most minerals. Second, we assume that bulk mineral-melt partitioning ($D_{Li}$) varies as a function of crystallization, from close to 1 at 0% crystallization to >10 at >90% crystallization. Progressive fractionation of a magma ocean leads to an increase in the $\delta^7Li$ value at $\alpha$ <1, where alpha is the equilibrium fractionation factor between melt and solid for $^7Li/^6Li$, assuming a bulk partition coefficient for the crystallizing minerals that is proportional to the mineral partition coefficient and the modal proportion of the mineral (Fig. 6). Under these conditions, $^{56}Fe/^{54}Fe$ (Weyer et al. 2005; Liu et al. 2010b) has been predicted to increase and $^{18}O/^{16}O$ to decrease (Spicuzza et al. 2007), in response to mineral-melt isotopic exchange during progressive fractional crystallization.

A key question is why this fractionation has not been observed before in basaltic systems, such as in Kilauea lava lake (Tomascak et al. 1999), or in Hekla (Schuessler et al. 2009), and whether there is evidence for preferential enrichment of $^7Li$ during large-scale magmatic fractionation. During partial melting of Earth's mantle, there are no observable equilibrium isotopic effects between melts and peridotites for Li (e.g., Rudnick and Ionov 2007; Magna et al. 2008). No fractionations that can be definitively attributed to high-temperature magmatic processes have been noted in Martian or howardiite–eucrite–diogenite meteorites (Magna et al. 2014, 2015). Likewise, the evidence for equilibrium fractionation of Li isotopes between melts and crystals is not well defined. Previous work has examined Li isotopic fractionation between minerals and fluids, observing $\delta^7Li$ fractionations of ~1‰ at temperatures of ~900 °C (Wunder et al. 2006). To our knowledge at present, no experimental examination of Li isotopic fractionation between melt and mineral at anhydrous conditions has been performed. Our results empirically suggest equilibrium fractionation factors between melt and solid for $^7Li/^6Li$ of >0.996, indicating

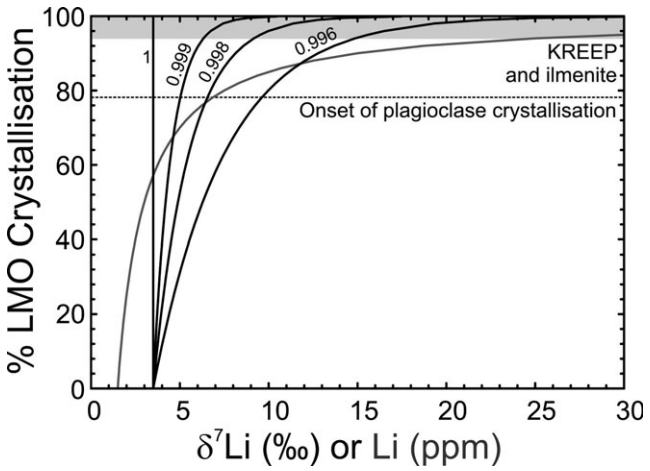


Fig. 6. Rayleigh distillation model for lithium and lithium isotopic composition in the Moon, as a function of lunar magma ocean (LMO) crystallization to illustrate the effect of isotopic fractionation (as different α-factors = 1, 0.999, 0.998, and 0.996) and the incompatible behavior of Li. $D_{Li}$ was allowed to vary in order to trace the degree of crystallization, starting at ~1, with >10 at >90% LMO crystallization. With increasing differentiation and even assuming the modest α-factors, the resulting melt is predicted to become enriched in the heavy isotopes of Li in conjunction with higher Li abundances. Shown for comparison is the approximate stage at which the onset of plagioclase (dashed line) and KREEP and high Fe-Ti oxide (ilmenite; shaded region) in the LMO are considered to have crystallized (e.g., Snyder et al. 1992).

that extensive fractional crystallization is required to produce observable effects on $\delta^7$Li.

Given these considerations, there are a number of potential reasons why Li isotopic fractionation during high-temperature igneous processes has not been previously observed. First, the role of water contents in moderating stable isotopic fractionation in magmas is not constrained, but may be important in moderating $^7$Li/$^6$Li fractionation between minerals and melt (e.g., Wunder et al. 2006). This effect may be similar to that recently proposed for fractionation of Si isotopes in lunar rocks (Poitrasson and Zambardi 2015). Anhydrous lunar magmas may preserve Li isotopic fractionation effects more readily than water-bearing terrestrial magmas. Second, the contrast in $\delta^7$Li between high- and low-Ti mare basalt may reflect the extreme scale of the differentiation process. It is possible that significant Li isotopic fractionations (exceeding typical analytical uncertainties) only become manifested in large-scale systems (i.e., global magma oceans) and at extreme degrees of fractional crystallization. The scale of the differentiation process (cf. lunar magma ocean [$>10 \times 10^{18}$ m$^3$] versus Kilauea lava lake [$44 \times 10^6$ m$^3$] or laboratory experiments [$\ll 0.1$ m$^3$]), water content, and external analytical reproducibility are potentially important factors in recognition of high-temperature Li isotopic fractionations.

An example of such a scaling effect may be present in the lunar data. LaPaz mare basalt meteorites are interpreted to result from fractional crystallization of parental melts similar in composition to those of the low-Ti Apollo 12 mare basalts (e.g., Righter et al. 2005; Zeigler et al. 2005; Day et al. 2006; Joy et al. 2006; Rankenburg et al. 2007). The higher Li concentrations in LaPaz mare basalts, relative to Apollo 15 low-Ti mare basalts, are therefore an expected consequence of fractional crystallization of parental magmas, whereas their match in $\delta^7$Li to Apollo 15 low-Ti mare basalts supports their identity as more evolved melts from a low-Ti mare basalt source formed by magma ocean processes (Fig. 2). In contrast, studies of KREEP-rich rocks 14310 (impact-melt rock), 15445 (breccia), 65015 and 62235 (poikilitic impact melt breccias) show consistently high Li contents, but a surprisingly wide range in $\delta^7$Li (1.9–18.4‰) (Seitz et al. 2006; Magna et al. 2009). To date, no definitively "pristine" KREEP-rich basalts (e.g., 15382/15386) have been measured for $\delta^7$Li. Nonetheless, the heavy isotopic compositions of some KREEP-rich breccias are consistent with the model presented here, supporting increasing $\delta^7$Li with progressive fractional crystallization of a magma ocean.

Simple assumptions of Li isotopic fractionation during differentiation of a lunar magma ocean under a particular fractionation factor (α) suggest that minerals crystallizing later will have higher $\delta^7$Li and, depending on their affinity for Li, higher concentrations (Fig. 6). Early-formed cumulates should have lower $\delta^7$Li than ferroan anorthosites, and in turn, late-stage Fe-Ti oxide and incompatible element-rich layers should have the highest $\delta^7$Li and Li contents. For example, ilmenite- and incompatible-element-rich cumulates, thought to form at ~95% magma ocean solidification (Snyder et al. 1992), would have $\delta^7$Li >6‰ using an initial silicate Moon composition close to the composition of chondrites. Any resolvable differences in Li isotope compositions between high- and low-Ti mare basalts would also potentially constrain the amount of remixing of Ti-rich materials into the lunar mantle, as required from phase equilibria of low- and high-Ti basalts. We have constructed models in order to estimate the proportions of ilmenite in mare basalt mantle sources, since this mineralogical indicator is a major distinction between low- and high-Ti mare basalts.

Mixing models were constructed between a primitive, early-formed cumulate reservoir (e.g., early mafic silicates responsible for low-Ti mare basalts) and late-stage lunar magma ocean crystallization products (LMOX) that experienced fractionation of Li (α) and are rich in Fe-Ti and incompatible elements (e.g.,

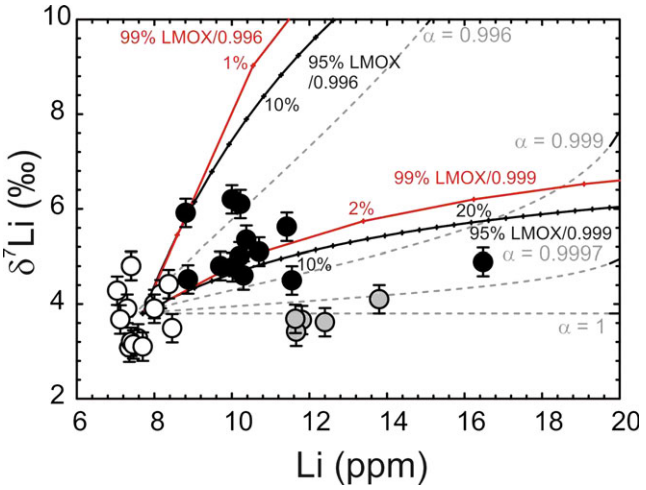


Fig. 7. Theoretical calculation of the proportions of ilmenite in high-Ti mare basalt mantle sources using end-member compositions estimated from modeling of Li isotopic and elemental evolution in the lunar magma ocean. For example, 95% LMOX/0.996 indicates mixing between a primitive, early-formed cumulate reservoir with a 95% crystallized lunar magma ocean (LMOX) product using an α-factor of 0.996. Also shown as gray stippled lines are Rayleigh fractionation models, as shown in Fig. 6. Mixing between variably crystallized mantle reservoirs is required to explain the Li isotopic and elemental abundances of mare basalts. An alpha factor of unity would be consistent with fractional crystallization unaccompanied by isotopic fractionation, as indicated by fractionation typically experienced by terrestrial magmatic systems and from the difference between low-Ti Apollo 15 mare basalts and the evolved low-Ti LaPaz mare basalt meteorites. Tick marks are in 1% increments.

urKREEP; Fig. 7). LMOX can be restricted to 10–20% of high-Ti mare basalt reservoirs, assuming LMOX after 95% magma ocean crystallization, and α between 0.996 and 0.999. Smaller fractions of LMOX are required in such a model (1–2%), if formed by greater degrees of magma ocean crystallization (>99%). These models naturally predict lower Li concentrations and lower $\delta^7$Li in early-formed magma ocean cumulates and the inverse for LMOX. The proportion of mixing between LMOX and early-formed cumulate reservoirs also implies lower $\delta^{18}$O and higher $\delta^{56}$Fe in late-stage magma ocean cumulates (e.g., Spicuzza et al. 2007; Liu et al. 2010b). While numerous aspects of our understanding of Li behavior during crystallization and melting remain poorly constrained, significant stable isotope fractionations (e.g., Li-O-Fe) appear to have occurred during large-scale high-temperature differentiation, under nominally anhydrous conditions in the Moon. This conclusion is consistent with a lunar magma ocean origin for the generation of elemental (e.g., Eu) and stable isotopic variability observed in the Moon.

### Planetary Magma Oceans and Chondritic Li Variations

Of the mare basalts, it is the low-Ti varieties that offer the best proxies for the lunar mantle $\delta^7$Li composition. This assertion is supported by three primary lines of evidence. First, magma ocean differentiation models predict that the largest reservoirs in the lunar mantle are early-formed olivine and orthopyroxene cumulates from which low-Ti mare basalts derive (Snyder et al. 1992; Warren and Taylor 2014). Second, remote sensing studies of the lunar surface show a preponderance (~90%) of low-Ti mare basalt compositions over high-Ti mare basalts (Giguere et al. 2000). Third, calculated $\delta^{18}$O of olivine between low-Ti mare basalts and MORB is identical (Spicuzza et al. 2007), implying similarities between the two most voluminous reservoirs accessible from partial melt products in Earth and the Moon. Planetary basalts show a similar range of Li abundances and overlap in Li isotopic compositions. On average, $\delta^7$Li of these planetary basalts, at ~4‰, is in the range of whole-rock terrestrial mantle peridotites, but is isotopically heavier than most chondrites (Fig. 8).

Lithium isotope compositions differ between carbonaceous, ordinary, and enstatite chondrites, with CI1, CV3, and CO3 chondrites being some of the most isotopically heavy of all the chondrite groups, due to parent body aqueous alteration (e.g., Seitz et al. 2007; Sephton et al. 2004, 2013). Conversely, ordinary and enstatite chondrites, with higher petrological grade, have generally lower $\delta^7$Li, but may also have experienced modification on their parent body (e.g., Pogge von Strandmann et al. 2011). These factors potentially limit the utility of Li isotopes for comparing potential building blocks of planets; lithium's effectiveness at tracing water-rock interactions and high-temperature fractionation effects in anhydrous bodies may limit its utility in studies of the building blocks of planets.

## CONCLUSIONS

Lithium isotopic differences between low- and high-Ti mare basalts can be explained through extensive high-temperature igneous fractionation, likely during magma ocean crystallization of the Moon. The abundances and isotopic compositions of lunar, terrestrial, Martian, and vestan basalts (i.e., eucrites) are all isotopically heavier than the average for chondrites (2.1 ± 1.3‰). Assumed isotopic enrichment of $^7$Li in melts and crystallization of a lunar magma ocean led to $^7$Li/$^6$Li fractionation. From these observations, it is possible to explain fractionations in Li, O, and Fe isotopes in low-Ti and high-Ti mare basalt mantle

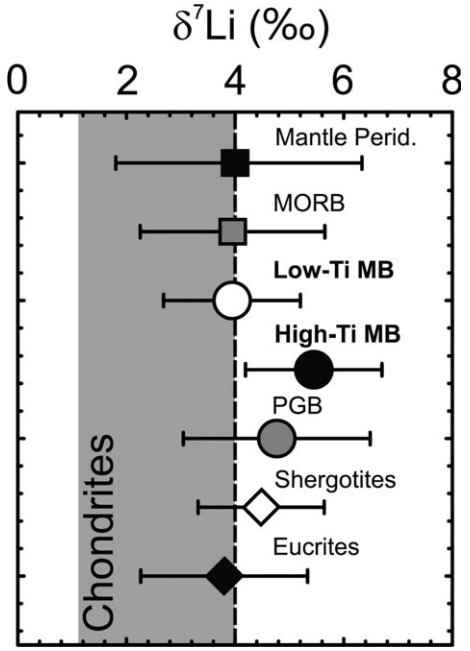


Fig. 8. Average $\delta^7$Li and 2σ standard deviations for mantle-derived partial melts from the Moon (low- and high-Ti mare basalts [MB] and pyroclastic glass beads [PGB]), Earth (MORB), Mars (Shergottites), and the eucrite parent body versus terrestrial mantle peridotites (Mantle Perid.), and the gray-shaded field for chondrites (2.1 ± 1.3‰), extending to the highest $\delta^7$Li measured in CI-chondrite, Orgueil. The dashed line is the average composition of bulk-rock terrestrial mantle peridotites. Data sources include this study, Seitz et al. (2004, 2006, 2007, 2012); Magna et al. (2006, 2014, 2015); Elliott et al. (2006); Jeffcoate et al. (2007); Tomascak et al. (2008); Pogge von Strandmann et al. (2011).

sources (low-Ti mantle source: $\delta^7$Li ≤4‰; $\delta^{56}$Fe ≤0.04‰; $\delta^{18}$O ≥5.7‰; high-Ti mantle source: $\delta^7$Li >6‰; $\delta^{56}$Fe >0.18‰; $\delta^{18}$O <5.4‰) through formation of mineralogically distinct cumulate mantle sources formed during a lunar magma ocean phase. Magma ocean crystallization models, coupled with Li isotope variations in mare basalts, indicate enrichment in Li contents and $\delta^7$Li with increasing magmatic differentiation. Using the $\delta^7$Li of the high-Ti mare basalts, and a model assuming mixing between early magma ocean cumulates and late-stage magma ocean liquids after 95% fractionation, produces a model-dependent source that consists of a mixture of ~80% of a low-Ti mare basalt-like mantle source and ~20% late-stage Fe-Ti oxides and incompatible element-rich materials. The evidence for Li isotope fractionation in mare basalts suggests the need for experimental studies of lithium isotopic fractionation between minerals and basaltic melts under near-anhydrous conditions in order to understand better processes governing high-temperature differentiation events in planetary bodies. Further analysis of KREEPy samples for Li isotopes are also required, as the only available $\delta^7$Li for KREEP has been measured on impact-modified rocks and not KREEP-rich basalts. If magma ocean crystallization led to Rayleigh-type fractionation of Li isotopes, early-formed KREEP reservoirs should be isotopically heavy. Finally, other stable isotope systems (e.g., Si, Ca, Mg, Cr, V, and Cu) may show similar effects and elucidate mechanisms of stable isotopic fractionation during high-temperature igneous processes.

*Acknowledgments*—We thank X.-M. Liu for assistance in the laboratory at the University of Maryland and R.J. Walker for encouragement and support. J.-A. Barrat and P. Tomascak are thanked for extensive and helpful review comments during preparation of this article, and A. Ruzicka is thanked for careful editorial handling. This work was made possible through NASA Emerging Worlds (NNX15AL74G), NASA LASER (NNX11AG34G), and NASA Cosmochemistry funding (NNX12AH75G, NNX10AG94G, NNX11AG58G, NNG04GG176G), as well as NSF 0948549, which partially supported participation of LQ in this work. The authors declare no conflicts of interest.

*Editorial Handling*—Prof. Alex Ruzicka

## REFERENCES

Anand M., Taylor L. A., Floss C., Neal C. R., Terada K., and Tanikawa S. 2006. Petrology and geochemistry of LaPaz Icefield 02205: A new unique low-Ti mare-basalt meteorite. *Geochimica et Cosmochimica Acta* 70:246–264.

Andersen C. A., Hinthorne J. R., and Fredriksson K. 1970. Ion microprobe analysis of lunar material from Apollo 11. Proceedings, Apollo 11 Lunar Science Conference. pp. 159–167.

Barrat J. A., Chaussidon M., Bohn M., Gillet P., Göpel C., and Lesourd M. 2005. Lithium behaviour during cooling of a dry basalt: An ion-microprobe study of the lunar meteorite Northwest Africa 479 (NWA 479). *Geochimica et Cosmochimica Acta* 69:5597–5609.

Beck P., Chaussidon M., Barrat J. A., Gillet P., and Bohn M. 2006. Diffusion induced Li isotopic fractionation during the cooling of magmatic rocks: The case of pyroxene phenocrysts from nakhlites meteorites. *Geochimica et Cosmochimica Acta* 70:4813–4825.

Brearley A. J. and Jones R. H. 1998. Chondritic meteorites. *Reviews in mineralogy and geochemistry* 36(1):3.1–3.398.

Brenan J. M., Neroda F., Lundstrom C. C., Shaw H. E., Ryerson F. E., and Phinney D. J. 1998. Behaviour of boron, beryllium, and lithium during melting and crystallization: Constraints from mineral-melt partitioning experiments. *Geochimica et Cosmochimica Acta* 62:2129–2141.

Chan L. H. and Edmond J. M. 1988. Variation of lithium isotope composition in the marine environment: A preliminary report. *Geochimica et Cosmochimica Acta* 52:1711–1717.

Chappell B. W. and Green D. H. 1973. Chemical compositions and petrogenetic relationships in Apollo 15 mare basalts. *Earth and Planetary Science Letters* 18:237–246.

Chaussidon M. and Robert F. 1998. $^{7}Li/^{6}Li$ and $^{11}B/^{10}B$ variations in chondrules from the Semarkona unequilibrated chondrite. *Earth and Planetary Science Letters* 164:577–589.

Chaussidon M. and Robert F. 1999. Lithium nucleosynthesis in the Sun inferred from the solar-wind $^{7}Li/^{6}Li$ ratio. *Nature* 402:270–273.

Day J. M. D. and Moynier F. 2014. Evaporative fractionation of volatile stable isotopes and their bearing on the origin of the Moon. *Philosophical Transactions of the Royal Society A* 372:20130259.

Day J. M. D. and Taylor L. A. 2007. On the structure of mare basalt lava flows from textural analysis of the LaPaz icefield and Northwest Africa 032 lunar meteorites. *Meteoritics & Planetary Science* 42:3–18.

Day J. M. D. and Walker R. J. 2015. Highly siderophile element depletion in the Moon. *Earth and Planetary Science Letters* 423:114–124.

Day J. M. D., Taylor L. A., Floss C., Patchen A. D., Schnare D. W., and Pearson D. G. 2006. Comparative petrology, geochemistry, and petrogenesis of evolved, low-Ti lunar mare basalt meteorites from the LaPaz Icefield, Antarctica. *Geochimica et Cosmochimica Acta* 70:1581–1600.

Day J. M. D., Pearson D. G., and Taylor L. A. 2007. Highly siderophile element constraints on accretion and differentiation of the Earth-Moon system. *Science* 315:217–219.

Elkins-Tanton L. T., Van Orman J. A., Hager B. H., and Grove T. L. 2002. Re-examination of the lunar magma ocean cumulate overturn hypothesis: Melting of mixing is required. *Earth and Planetary Science Letters* 196:239–249.

Elliott T., Jeffcoate A., and Bouman C. 2004. The terrestrial Li isotope cycle: Light-weight constraints on mantle convection. *Earth and Planetary Science Letters* 220:231–245.

Elliott T., Thomas A., Jeffcoate A., and Niu Y. 2006. Lithium isotope evidence for subduction-enriched mantle in the source of mid-ocean-ridge basalts. *Nature* 443:565–568.

Eugster O. and Bernas R. 1971. B, Li, Mg and Ti isotopic abundances and search for trapped solar wind Li in Apollo 11 and Apollo 12 material. Proceedings, 2nd Lunar Science Conference. pp. 1461–1469.

Eugster O., Lorenzetti S., Krähenbühl U., and Marti K. 2007. Comparison of cosmic-ray exposure ages and trapped noble gases in chondrule and matrix samples of ordinary, enstatite, and carbonaceous chondrites. *Meteoritics & Planetary Science* 42:1351–1371.

Flesch G. D., Anderson A. R. Jr., and Svec H. J. 1973. A secondary isotopic standard for $^{6}Li/^{7}Li$ determinations. *International Journal of Mass Spectrometry and Ion Physics* 12:265–272.

Giguere T. A., Taylor G. J., Hawke B. R., and Lucey P. G. 2000. The titanium contents of lunar mare basalts. *Meteoritics & Planetary Science* 35:192–200.

Hill E., Taylor L. A., Floss C., and Liu Y. 2009. Lunar meteorite LaPaz Icefield 04841: Petrology, texture, and impact-shock effects of a low-Ti mare basalt. *Meteoritics & Planetary Science* 44:87–94.

Huh Y., Chan L. H., and Edmond J. M. 2001. Lithium isotopes as a probe of weathering processes: Orinoco River. *Earth and Planetary Science Letters* 194:189–199.

Jeffcoate A. B., Elliott T., Thomas A., and Bouman C. 2004. Precise, small sample size determination of lithium isotopic compositions in geological reference materials and modern seawater by MC-ICP-MS. *Geostandards and Geoanalytical Research* 28:161–172.

Jeffcoate A. B., Elliott T., Kasemann S. A., Ionov D., Cooper K., and Brooker R. 2007. Li isotope fractionation in peridotites and mafic melts. *Geochimica et Cosmochimica Acta* 71:202–218.

Jochum K. P. and Nohl U. 2008. Reference materials in geochemistry and environmental research and the GeoReM database. *Chemical Geology* 253:50–53.

Joy K. H., Crawford I. A., Downes H., Russell S. S., and Kearsley A. T. 2006. A petrological, mineralogical, and chemical analysis of the lunar mare basalt meteorite LaPaz Icefield 02205, 02224, and 02226. *Meteoritics & Planetary Science* 41:1003–1025.

Kato C., Moynier F., Valdes M., Dhaliwal J. K., and Day J. M. D. 2015. Extensive volatile loss during formation and differentiation of the Moon. *Nature Communications* 6:7617. doi:10.1038/ncomms8617.

Knauth D. C., Federman S. R., Lambert D. L., and Crane P. 2000. Newly synthesized lithium in the interstellar medium. *Nature* 405:656–658.

Liu X.-M., Rudnick R. L., Hier-Majumder S., and Sirbescu M. L. C. 2010a. Processes controlling lithium isotopic distribution in contact aureoles: A case study of the Florence County Pegmatites, Wisconsin. *Geochemistry, Geophysics, Geosystems* 11:8. doi:10.1029/2010GC003063.

Liu Y., Spicuzza M. J., Craddock P. R., Day J. M. D., Valley J. W., Dauphas N., and Taylor L. A. 2010b. Oxygen and iron isotope constraints on near-surface fractionation effects and the composition of lunar mare basalt source regions. *Geochimica et Cosmochimica Acta* 74:6249–6262.

Liu X.-M., Rudnick R. L., McDonough W. F., and Cummings M. L. 2013. Influence of chemical weathering on the composition of the continental crust: Insights from Li and Nd isotopes in bauxite profiles developed on Columbia River Basalts. *Geochimica et Cosmochimica Acta* 115:73–91.

Magna T., Wiechert U., and Halliday A. N. 2006. New constraints on the lithium isotope compositions of the Moon and terrestrial planets. *Earth and Planetary Science Letters* 243:336–353.

Magna T., Ionov D. A., Oberli F., and Wiechert U. 2008. Links between mantle metasomatism and lithium isotopes: Evidence from glass-bearing and cryptically metasomatised xenoliths from Mongolia. *Earth and Planetary Science Letters* 276:214–222.

Magna T., Neal C. R., Tomascak P. B., Bourdon B., Oberli F., and Day J. M. D. 2009. On lithium isotope systematics and abundances in lunar mare basalts. *Geochimica et Cosmochimica Acta* 73:A816.

Magna T., Simcikova M., and Moynier F. 2014. Lithium systematics in howardite-eucrite-diogenite meteorites: Implications for crust-mantle evolution of planetary embryos. *Geochimica et Cosmochimica Acta* 125:131–145.

Magna T., Day J. M. D., Mezger K., Fehr M. A., Channaoui-Aoudjehane H., and Agee C. 2015. Lithium isotope constraints on crust-mantle interactions and surface processes on Mars. *Geochimica et Cosmochimica Acta* 162:46–65.

Maruyama S., Watanabe M., Kunihiro T., and Nakamura E. 2009. Elemental and isotopic abundances of lithium in

chondrule constituents in the Allende meteorite. *Geochimica et Cosmochimica Acta* 73:778–793.

Meyer C. 2012. Lunar sample compendium. http://curator.jsc.nasa.gov/Lunar/lsc/index.cfm

Mittlefehldt D. W. 2005. Achondrites. In *Meteorites, comets and planets*, edited by Davis A. M. Treatise on Geochemistry vol. 1, Amsterdam: Elsevier. pp. 1–40.

Neal C. R. and Taylor L. A. 1992. Petrogenesis of mare basalts—A record of lunar volcanism. *Geochimica et Cosmochimica Acta* 56:2177–2211.

Paniello R. C., Day J. M. D., and Moynier F. 2012. Zinc isotopic evidence for the origin of the Moon. *Nature* 490:376–379.

Parkinson I. J., Hammond S. J., James R. H., and Rogers N. W. 2007. High-temperature lithium isotope fractionation: Insights from lithium isotope diffusion in magmatic systems. *Earth and Planetary Science Letters* 257:609–621.

Plank T. and Langmuir C. 1992. Effects of the melting regime on the composition of the oceanic crust. *Journal of Geophysical Research* 97:19,749–19,770.

Pogge von Strandmann P. A. E., Elliott T., Marschall H. R., Coath C., Lai Y. J., Jeffcoate A. B., and Ionov D. A. 2011. Variations of Li and Mg isotope ratios in bulk chondrites and mantle xenoliths. *Geochimica et Cosmochimica Acta* 75:5247–5268.

Poitrasson F. and Zambardi T. 2015. An Earth-Moon silicon isotope model to track silicic magma origins. *Geochimica et Cosmochimica Acta* 167:301–312.

Poitrasson F., Halliday A. N., Lee D. C., Levasseur S., and Teutsch N. 2004. Iron isotope differences between Earth, Moon, Mars and Vesta as possible records of contrasted accretion mechanisms. *Earth and Planetary Science Letters* 223:253–266.

Qiu L., Rudnick R. L., Ague J. J., and McDonough W. F. 2011. A lithium isotopic study of sub-greenschist to greenschist facies metamorphism in an accretionary prism, New Zealand. *Earth and Planetary Science Letters* 301:213–221.

Rankenburg K., Brandon A. D., and Norman M. D. 2007. A RbSr and SmNd isotope geochronology and trace element study of lunar meteorite LaPaz Icefield 02205. *Geochimica et Cosmochimica Acta* 71:2120–2135.

Rhodes J. M. and Hubbard N. J. 1973. Chemistry, classification, and petrogenesis of Apollo 15 mare basalts. Proceedings, 4th Lunar Science Conference. pp. 1127–1148.

Righter K., Collins S. J., and Brandon A. D. 2005. Mineralogy and petrology of the LaPaz Icefield lunar mare basaltic meteorites. *Meteoritics & Planetary Science* 40:1703–1722.

Rudnick R. L. and Ionov D. 2007. Lithium elemental and isotopic disequilibrium in minerals from peridotite xenoliths from far-east Russia: Product of recent melt/fluid–rock reaction. *Earth and Planetary Science Letters* 256:278–293.

Rudnick R. L., Tomascak P. B., Njo H. B., and Gardner R. L. 2004. Extreme isotopic fractionation during continental weathering revealed in saprolites from South Carolina. *Chemical Geology* 212:45–57.

Schnare D. W., Day J. M. D., Norman M. D., Liu Y., and Taylor L. A. 2008. A laser-ablation ICP-MS study of Apollo 15 low-titanium olivine-normative and quartz-normative mare basalts. *Geochimica et Cosmochimica Acta* 72:2556–2572.

Schuessler J. A., Schoenberg R., and Sigmarsson O. 2009. Iron and lithium isotope systematics of the Hekla volcano, Iceland—Evidence for Fe isotope fractionation during magma differentiation. *Chemical Geology* 258:78–91.

Sedaghatpour F., Teng F. Z., Liu Y., Sears D. W. G., and Taylor L. A. 2013. Magnesium isotopic composition of the Moon. *Geochimica et Cosmochimica Acta* 120:1–16.

Seitz H.-M., Brey G. P., Lahaye Y., Durali S., and Weyer S. 2004. Lithium isotopic signatures of peridotite xenoliths and isotopic fractionation at high temperature between olivine and pyroxenes. *Chemical Geology* 212:163–177.

Seitz H.-M., Brey G. P., Weyer S., Durali S., Ott U., Munker C., and Mezger K. 2006. Lithium isotope compositions of Martian and lunar reservoirs. *Earth and Planetary Science Letters* 245:6–18.

Seitz H.-M., Brey G. P., Zipfel J., Ott U., Weyer S., Durali S., and Weinbruch S. 2007. Lithium isotope composition of ordinary and carbonaceous chondrites, and differentiated planetary bodies: Bulk solar system and solar reservations. *Earth and Planetary Science Letters* 260:582–596.

Seitz H.-M., Zipfel J., Brey G. P., and Ott U. 2012. Lithium isotope compositions of chondrules, CAI and a dark inclusion from Allende and ordinary chondrites. *Earth and Planetary Science Letters* 329:51–59.

Sephton M. A., James R. H., and Bland P. A. 2004. Lithium isotope analyses of inorganic constituent from the Murchison meteorite. *The Astrophysical Journal* 612:588–591.

Sephton M. A., James R. H., Fehr M. A., Bland P. A., and Gounelle M. 2013. Lithium isotopes as indicators of meteorite parent body alteration. *Meteoritics & Planetary Science* 48:872–878.

Sharp Z. D., Shearer C. K., McKeegan K. D., Barnes J. D., and Wang Y. Q. 2010. The chlorine isotope composition of the Moon and implications for an anhydrous mantle. *Science* 329:1050–1053.

Shearer C. K. and Papike J. J. 1999. Magmatic evolution of the Moon. *American Mineralogist* 84:1469–1494.

Shearer C. K., Sharp Z. D., Burger P. V., McCubbin F. M., Provencio P. P., Brearley A. J., and Steele A. 2014. Chlorine distribution and its isotopic composition in "rusty rock" 66095. Implications for volatile element enrichments of "rusty rock" and lunar soils, origin of "rusty" alteration, and volatile element behavior on the Moon. *Geochimica et Cosmochimica Acta* 139:411–433.

Smith J. A., Anderson A. T., Newton R. C., Olsen E. J., Wyllie P. J., Crewe A. V., Isaacson M. S., and Johnson D. 1970. Petrologic history of the Moon inferred from petrography, mineralogy, and petrogenesis of Apollo 11 rocks. Proceedings, Apollo 11 Lunar Science Conference. pp. 1149–1162.

Snyder G. A., Taylor L. A., and Neal C. R. 1992. A chemical model for generating the sources of mare basalts: Combined equilibrium and fractional crystallization of the lunar magmasphere. *Geochimica et Cosmochimica Acta* 56:3809–3824.

Snyder G. A., Neal C. R., Taylor L. A., and Halliday A. N. 1997. Anataxis of lunar cumulate mantle in time and space. Clues from trace-element, strontium and neodymium isotopic chemistry of parental Apollo 12 basalts. *Geochimica et Cosmochimica Acta* 61:2731–2747.

Spicuzza M. J., Day J. M. D., Taylor L. A., and Valley J. W. 2007. Oxygen isotope constraints on the origin and differentiation of the Moon. *Earth and Planetary Science Letters* 253:254–265.

Teng F.-Z., McDonough W. F., Rudnick R. L., Dalpe C., Tomascak P. B., Chappell B. W., and Gao S. 2004. Lithium isotopic composition and concentration of the upper continental crust. *Geochimica et Cosmochimica Acta* 68:4167–4178.

Teng F. Z., McDonough W. F., Rudnick R. L., and Walker R. J. 2006. Diffusion-driven extreme lithium isotopic fractionation in country rocks of the Tin Mountain pegmatite. *Earth and Planetary Science Letters* 243:701–710.

Tomascak P. B. 2004. Developments in the understanding and application of lithium isotopes in the earth and planetary sciences. *Reviews in Mineralogy and Geochemistry* 55:153–195.

Tomascak P. B., Tera F., Helz R. T., and Walker R. J. 1999. The absence of lithium isotope fractionation during basalt differentiation: New measurements by multicollector sector ICP-MS. *Geochimica et Cosmochimica Acta* 63:907–910.

Tomascak P. B., Langmuir C. H., le Roux P. J., and Shirey S. B. 2008. Lithium isotopes in global mid-ocean ridge basalts. *Geochimica et Cosmochimica Acta* 72:1626–1637.

Van Kan Parker M., Mason P. R. D., and Van Westrenen W. 2011. Experimental study of trace element partitioning between lunar orthopyroxene and anhydrous silicate melt: Effects of lithium and iron. *Chemical Geology* 285:1–14.

Warren P. H. and Taylor G. J. 2014. The Moon. In *Treatise on geochemistry*, edited by Davis A. M. Amsterdam: Elsevier. pp. 213–242.

Weyer S., Anbar A. D., Brey G. P., Munker C., Mezger K., and Woodland A. B. 2005. Iron isotope fractionation during planetary differentiation. *Earth and Planetary Science Letters* 240:251–264.

Wiechert U. and Halliday A. N. 2007. Non-chondritic magnesium and the origins of the inner terrestrial planets. *Earth and Planetary Science Letters* 256:360–371.

Wood J. A., Dickey J. S., Marvin U. B., and Powell B. N. 1970. Lunar anorthosites and a geophysical model of the Moon. Proceedings, Apollo 11 Lunar Science Conference. pp. 965–988.

Wunder B., Meixner A., Romer R. L., and Heinrich W. 2006. Temperature-dependent isotopic fractionation of lithium between clinopyroxene and high-pressure hydrous fluids. *Contributions to Mineralogy and Petrology* 151:112–120.

Zack T., Tomascak P. B., Rudnick R. L., Dalpe C., and McDonough W. F. 2003. Extremely light Li in orogenic eclogites: The role of isotope fractionation during dehydration in subducted oceanic crust. *Earth and Planetary Science Letters* 208:279–290.

Zeigler R. A., Korotev R. L., Jolliff B. L., and Haskin L. A. 2005. Petrography and geochemistry of the LaPaz Ice Field basaltic lunar meteorite and source-crater pairing with Northwest Africa 032. *Meteoritics & Planetary Science* 40:1073–1102.

## SUPPORTING INFORMATION

Additional supporting information may be found in the online version of this article:

**Fig S1.** Measured Li concentration in whole rocks versus the calculated whole-rock Li concentration from modal recombination using measured Li in plagioclase, pyroxene, olivine, ilmenite, and silica in Apollo 15555, 955. The plot serves to illustrate that LaPaz and Apollo 17 mare basalt samples require a phase, or phases, with higher concentrations of Li than measured in 15555. The identity of these phases is currently unresolved, but may include armalcolite.

**Table S1.** Data for 50 ppm standard solutions UMD-1 and IRMM 016.

**Table S2.** Li isotope and abundance data for standards BHVO-2 and JB-2.

**Table S3.** Published values for Standard Reference Materials used in this study.

**Table S4.** Summary of Li isotope and abundance data for mare basalts.